

Geometrical scaling of prompt photons in heavy ion collisions

Michał Praszalowicz^{1,*}

¹M. Smoluchowski Institute of Physics, Jagiellonian University, S. Łojasiewicza 11, 30-348 Kraków, Poland

Abstract. We discuss geometrical scaling (GS) for the prompt (direct) photons produced in heavy ion collisions. To this end we first introduce the concept of GS and illustrate its emergence on the example of charged particles. Next, we analyse direct photon data from RHIC and from the LHC. We show that the data support the hypothesis of GS in terms of participant number related to different centrality classes. We also study GS at different energies, however a more detailed study will be possible only when data for at least three different energies from one experiment will be available and also when we use the data obtained from the collisions of large systems (Cu+Cu, Au+Au, Pb+Pb) and small systems (p+p, d+Au, p+Au).

1 Introduction

It is now widely accepted that in high energy scattering the bulk features of the produced particles spectra give access to the properties of the initial state. Especially, in the small Bjorken x kinematical region, where the initial hadrons consist predominantly from the overoccupied gluonic cloud, a phenomenon called *geometrical scaling* (GS) arises. Geometrical scaling has been first observed in the inclusive deep inelastic electron-proton scattering (DIS) [1], where the reduced cross section, essentially $F_2(x, Q^2)/Q^2$, which is in principle a function of two variables x and Q^2 , depends in fact on only one scaling variable $\tau = Q^2/Q_{\text{sat}}^2(x)$. The saturation scale

$$Q_{\text{sat}}^2(x) = Q_0^2 (x/x_0)^{-\lambda} \quad (1)$$

is directly proportional to the gluon density in the proton, and x_0 and Q_0 are fixed parameters of the order of 10^{-3} and 1 GeV/ c , respectively. Exponent $\lambda \approx 0.33$ is a nonperturbative dynamical quantity following from the properties of the (non-linear) QCD evolution equation, however its numerical value has to be fixed from the data (for review see Ref. [2]).

The properties of the saturated gluon densities should have an impact on the particles produced in proton-proton collisions. Indeed, adopting a so called parton-hadron duality [3], one can argue that the bulk properties of the gluon spectra are shared by charged particles that are eventually detected experimentally. In particular they exhibit GS in the small x region (*i.e.* large energy \sqrt{s} and moderate p_T) [4, 5]. However, multiplicity spectra scale with a somewhat lower power λ than the one extracted from DIS. We have argued that for pp scattering, where one does not control the overlap area transverse to the center of mass reaction axis, the quantity that scales with $\lambda \approx 0.33$ is the differential cross

*e-mail: michal@if.uj.edu.pl

section, rather than multiplicity [6]. This should be contrasted with the heavy ion (HI) reactions, when the transverse overlap area is controlled by an appropriate choice of centrality classes.

The fact that GS exhibited by the gluons is transferred to the final state particles, which are created in the nonperturbative hadronization process, which undergo final state interactions, which are being produced by resonance decays, is by no means obvious. This is even more so in the case of HI collisions where the quark-gluon plasma (QGP) is created and undergoes hydrodynamical evolution. Nevertheless, following Refs. [7, 8], we will show in the next section that GS in charged particles spectra is indeed present even in this case.

From this point of view direct photons (by definition photons that do not originate from hadronic decays) are an excellent probe of the initial state of HI collisions since they do not interact strongly while passing through the quark-gluon plasma. However, photons are produced from quarks (through annihilation and Compton scattering), and therefore they do not probe the overoccupied gluonic cloud directly. To this end one employs the Color Glass Condensate (CGC) effective theory where the initial gluonic CGC evolves into an intermediate state called glasma, which is a strongly interacting not thermalised QGP [2]. Quarks are produced in the thermalisation process, and – if there are no other mass scales around – their distribution should exhibit geometrical scaling¹ in variable $\tau = p_T^2/Q_{\text{sat}}^2(x)$. Similarly, the photon spectra should scale as well. In order to validate this scenario one should check if the available photon data exhibit geometrical scaling. The first step in this direction has been undertaken in Ref. [12] where the functional form of the photon spectra has been assumed to be of the form p_T^{-n} (see also Refs. [9–11]). Here, following Refs. [4–8], we shall employ model independent *method of ratios* to analyse GS of photon spectra, which is done in Sect. 3. But first, in Sect. 2, we shortly recall analysis of charged particle spectra already reported in Refs. [7, 8]. We conclude in Sect. 4.

2 Charged particles

By geometrical scaling [1] of charged particles in hadronic collisions we mean that the multiplicity distributions are well described – up to the logarithmic correction of the running coupling constant – by a universal function $F(\tau)$ [4, 5]:

$$\frac{1}{S_{\perp}} \frac{dN_{\text{ch}}}{d\eta d^2p_T} = F(\tau) \quad (2)$$

of the scaling variable

$$\tau = \frac{p_T^2}{Q_{\text{sat}}^2}. \quad (3)$$

Saturation scale (for particles produced in mid rapidity region) reads therefore

$$Q_{\text{sat}}^2 = Q_0^2 \left(\frac{p_T}{W x_0} \right)^{-\lambda}. \quad (4)$$

Here $W = \sqrt{s}$ is the scattering energy and for the reference we take $x_0 = 10^{-3}$ and $Q_0 = 1 \text{ GeV}/c$. Parameter S_{\perp} is a transverse area, which for heavy ion collisions corresponds to geometrical overlap of the colliding nuclei at given impact parameter b [13]. HI data are usually divided into centrality classes that select events within certain range of impact parameter b . In this case both transverse area

¹Detailed description of the photon production mechanism in glasma is beyond scope of this report; we refer the reader to Refs. [9–11].

S_{\perp} and the saturation scale Q_{sat}^2 acquire additional dependence on centrality that is characterized by an average number of participants N_{part} . We have [12, 13]:

$$S_{\perp} \sim N_{\text{part}}^{\delta} \quad \text{and} \quad Q_{\text{sat}}^2 \sim N_{\text{part}}^{\delta/2}. \quad (5)$$

where one typically assumes $\delta = 2/3$, which follows from the collision geometry. Therefore in HI collisions

$$\frac{1}{N_{\text{evt}} N_{\text{part}}^{\delta}} \frac{dN_{\text{ch}}}{2\pi p_{\text{T}} d\eta dp_{\text{T}}} = \frac{1}{Q_0^2} F(\tau) \quad (6)$$

and the scaling variable τ takes the following form:

$$\tau = \frac{p_{\text{T}}^2}{N_{\text{part}}^{\delta/2} Q_0^2} \left(\frac{p_{\text{T}}}{W} \right)^{\lambda}. \quad (7)$$

Taking $x_0 = 10^{-3}$ we have that the energy W should be expressed in TeV, whereas p_{T} in GeV. The analysis presented here will be only qualitative and we shall not fine tune the scaling exponent λ keeping it fixed at $\lambda = 0.3$.

In this section we shall analyse ALICE data on PbPb collisions at 2.76 TeV [14] and also earlier data from RHIC from STAR [15, 16] and PHENIX [17, 18] collaborations at 200 and 130 GeV per nucleon respectively. Centrality classes together with participants numbers are given in Table 1.

Table 1. Centrality classes and the corresponding numbers of participants in heavy ion experiments analysed in this paper. Energies per nucleon in TeV are displayed next to the experiment name. Bold face entries in blue (color on-line) show classes of similar number of participants analysed in the text.

| ALICE 2.76 | | STAR 0.2 & 0.13 | | PHENIX 0.2 | | PHENIX 0.13 | |
|---------------|-------------------|-----------------|-------------------|---------------|-------------------|---------------|-------------------|
| centrality | N_{part} | centrality | N_{part} | centrality | N_{part} | centrality | N_{part} |
| 0-5% | 383 | | | | | | |
| 5-10% | 330 | 0-5% | 350 | 0-10% | 352.2 | 0-5% | 348 |
| | | 5-10% | 296 | | | 5-15% | 271 |
| 10-20% | 261 | 10-20% | 232 | 10-20% | 234.6 | | |
| 20-30% | 186 | 20-30% | 165 | 20-30% | 166.6 | 15-30% | 180 |
| 30-40% | 129 | 30-40% | 115 | 30-40% | 114.2 | | |
| 40-50% | 85 | | | 40-50% | 74.4 | 30-60% | 79 |
| 50-60% | 53 | 40-60% | 62 | 50-60% | 45.5 | | |
| 60-70% | 30 | 60-80% | 20 | 60-70% | 25.7 | 60-80% | 19.5 |
| 70-80% | 15.8 | | | 70-80% | 13.4 | | |
| | | | | 80-92% | 6.3 | 80-92% | 5.5 |

In Fig. 1 we plot multiplicity distributions from all three experiments displayed in Table 1, for different centrality classes and – in the case of STAR and PHENIX – for both scattering energies. First in the left panel multiplicity distributions are plotted as functions of p_{T} and then in the right panel as functions of scaling variable $\sqrt{\tau}$ (7). We see that different distributions from the left panel coincide over some range of $\sqrt{\tau}$ when scaled according to Eq. (6). For clarity in Fig. 1 we have used only every second centrality class of ALICE and PHENIX@200 GeV data.

We can see from Fig. 1 that, indeed, heavy ion data scale according to (6) up to $\sqrt{\tau} \sim 1.8$ approximately. The quality of scaling is, however, not as good as in the case of pp scattering [5]. One could perhaps improve the quality of GS by tuning the exponent λ in the definition of τ (7). We have

decided to keep λ constant for the purpose of present analysis because of the systematic differences between the data from different collaborations. The data has been taken in the rapidity intervals that are different in different experiments, also the partition of the data into centrality classes varies from one experiment to another as can be seen from Table 1.

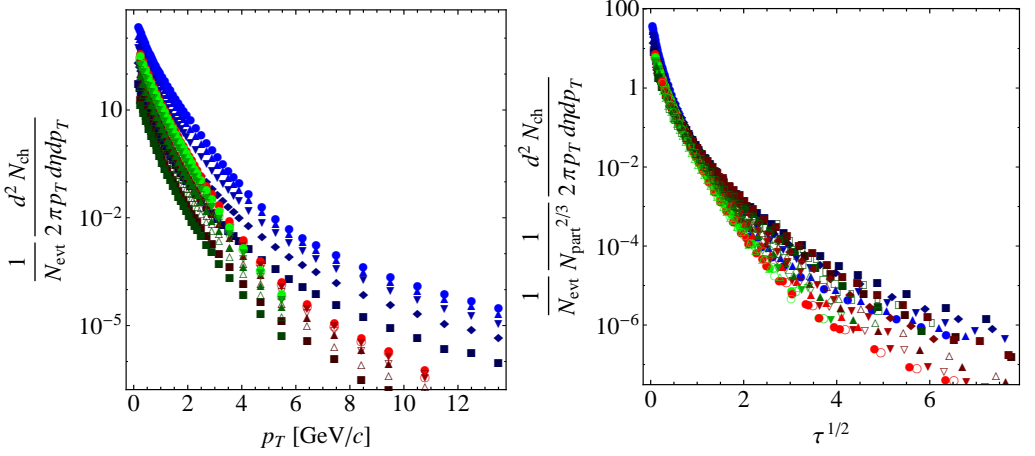


Figure 1. Illustration of geometrical scaling in heavy ion collisions at different energies and different centrality classes. Left panel shows charged particle distributions from ALICE [14], STAR [15, 16] and PHENIX [17, 18] plotted as functions of p_T . In the right panel the same distributions are scaled according to Eq. (6). Symbols used here are the same as in Figs. 2–3.

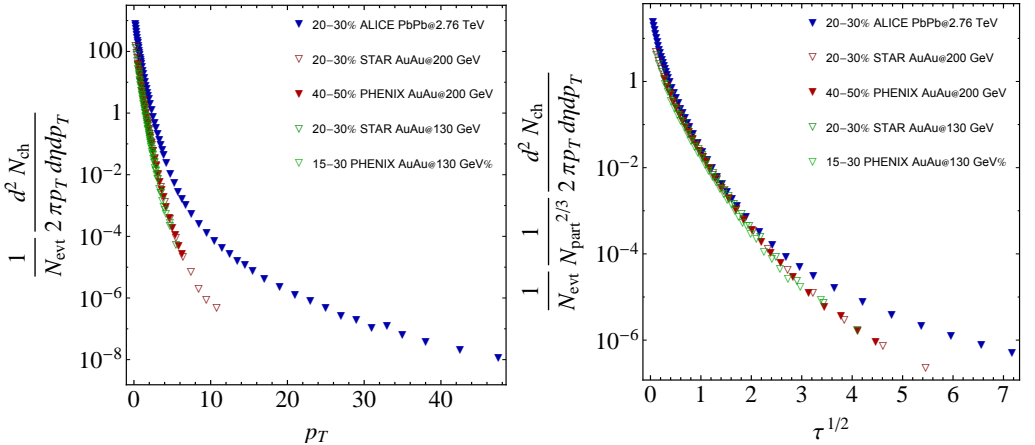


Figure 2. Illustration of geometrical scaling in heavy ion collisions at different energies for mid centrality classes corresponding to $n_{\text{part}} = 165 - 186$. Left panel shows charge particle distributions from ALICE [14], STAR [15, 16] and PHENIX [17, 18] plotted as functions of p_T . In the right panel the same distributions are scaled according to Eq. (6).

It is interesting to test now the quality of GS separately in dependence on energy and on centrality (*i.e.* on N_{part}). Let us first discuss scaling with energy by selecting centrality classes that correspond to similar number of participants in all three experiments. For illustration we plot in Fig. 2 multiplicity distributions with $n_{\text{part}} = 165 - 186$ (second blue row in Table 1). We see rather good scaling up to $\sqrt{\tau} \approx 2$. The plots for other centralities look very much the same.

For fixed scattering energy W equation (6) relates distributions of different participant number. We shall now examine the quality of this scaling by plotting multiplicity distributions at the same energy but different centrality classes. In Fig. 3 we plot ALICE data at 2.76 GeV. Plots for RHIC energies are very similar, and one can say that generally centrality scaling is of worse quality than the energy scaling discussed above.

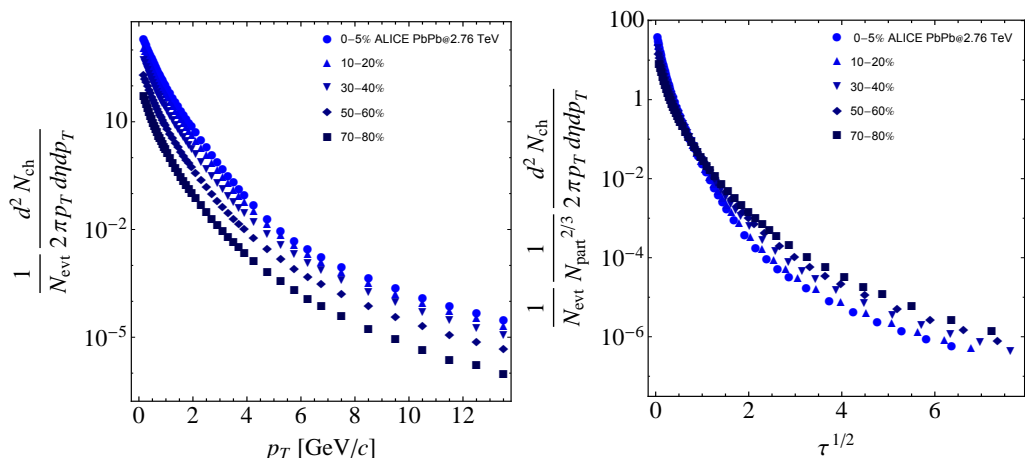


Figure 3. Illustration of geometrical scaling in heavy ion collisions at fixed ALICE [14] energy of 2.76 TeV for different centrality classes. Left panel shows charge particle distributions plotted as functions of p_T . In the right panel the same distributions are scaled according to Eq. (6).

3 Photons

In this paper we shall analyse the following data sets on direct photons: PHENIX [19, 20] Au+Au @ 200 GeV with the following centrality classes 0-20% ($N_{\text{part}} = 277.5$), 20-40% ($N_{\text{part}} = 135.6$), 40-60% ($N_{\text{part}} = 56.0$), 60-92% ($N_{\text{part}} = 12.5$) and ALICE² [21, 22] Pb+Pb @ 2.76 TeV: 0-20% ($N_{\text{part}} = 308$), 20-40% ($N_{\text{part}} = 157$) and 40-80% ($N_{\text{part}} = 45.7$). More recent PHENIX data [23] reported this year has not been available at the time of preparing this manuscript.

3.1 N_{part} scaling

Let us first examine the N_{part} dependence of geometrical scaling for the ALICE data [22]. These spectra are plotted in the left panel of Fig. 4, where we have included points with $p_T \leq 10$ GeV/c. In the right panel the same spectra are plotted after rescaling according to (6) for $\delta = 2/3$. We see that to a very good accuracy all three spectra coincide. This result should be contrasted with the charged particle scaling shown in Fig 3, which is of much worse quality. The same analysis is illustrated in Fig. 5 for PHENIX data [19, 20].

²Special thanks to Jacek Otwinowski for providing us with the pertinent values of N_{part} .

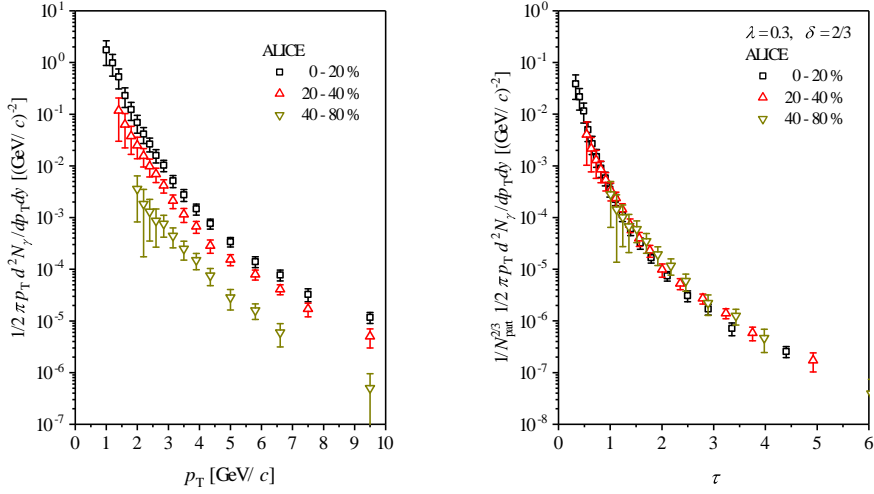


Figure 4. Illustration of N_{part} geometrical scaling of the γ yields in heavy ion collisions for different centrality classes for ALICE PbPb data. Left panel: transverse momentum spectra of direct photons at three centrality classes: 0-20% (black squares), 20-40% (red up-triangles), 40-80% (dark green down-triangles). Right panel: scaled spectra for $\delta = 2/3$. Data from Ref. [22].

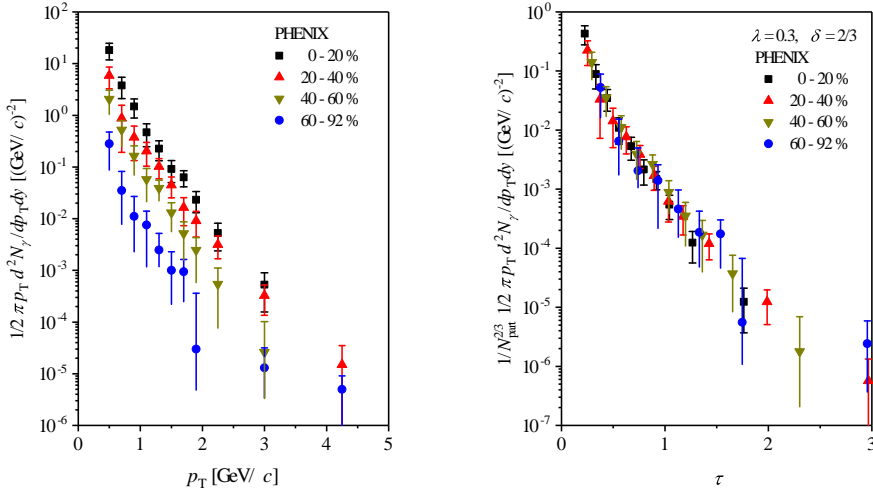


Figure 5. Illustration of N_{part} geometrical scaling of the γ yields in heavy ion collisions for different centrality classes for PHENIX AuAu data at 200 GeV [20]. Left panel: transverse momentum spectra of direct photons at four centrality classes: 0-20% (black squares), 20-40% (red up-triangle), 40-80% (dark green down-triangles), 6-92% (blue circles). Right panel: scaled spectra for $\delta = 2/3$. Lower error bars without end caps have been arbitrarily shortened for better visibility.

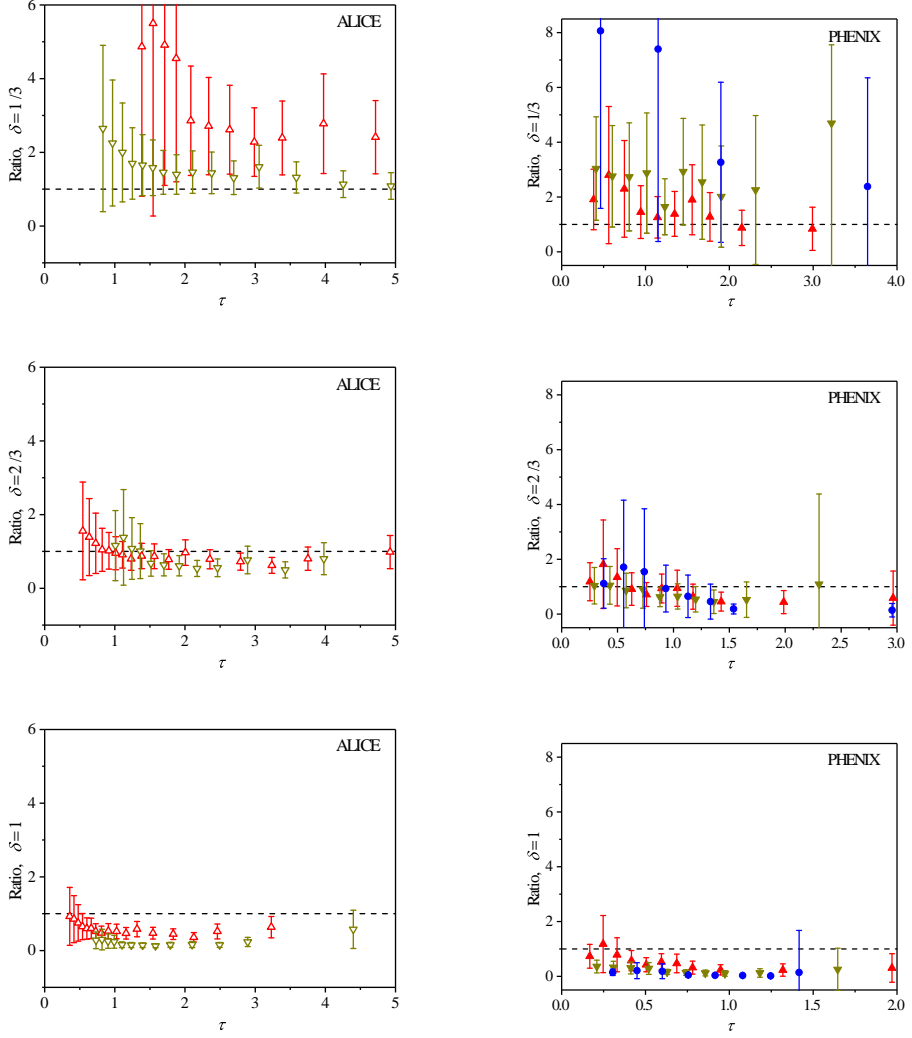


Figure 6. Illustration of geometrical scaling of the γ yields in heavy ion collisions at different centrality classes. Left panel: ALICE. Red triangles correspond to R_{c_1/c_2} and dark-green ones to R_{c_1/c_3} . Right panel: PHENIX. Red triangles points correspond to R_{c_1/c_2} , dark-green ones to R_{c_1/c_3} and blue ones to R_{c_1/c_4} . Upper plot $\delta = 1/3$, middle plot $\delta = 2/3$ and the lower plot $\delta = 1$.

In order to examine the quality of N_{part} scaling we construct the ratios of the scaled spectra at different centralities c_1 and c_2 , c_3 or c_4

$$R_{c_1/c_{2,3}}(\tau) = \frac{1}{N_{1\text{ part}}^\delta} \frac{dN_\gamma^{(1)}}{N_{\text{evt}} 2\pi p_T d\eta dp_T}(\tau) \bigg/ \frac{1}{N_{2,3\text{ part}}^\delta} \frac{dN_\gamma^{(2,3)}}{N_{\text{evt}} 2\pi p_T d\eta dp_T}(\tau) \quad (8)$$

and plot them for different δ as functions τ in Fig. 6. In the left panel we plot ALICE data where red up-triangles points correspond to $c_2 = 20 - 40\%$ and the dark green down-triangles to $c_3 = 40 - 80\%$. Geometrical scaling is achieved when $R_{c_1/c_2} \approx R_{c_1/c_3} \sim 1$. As one can see from Fig. 6, this happens indeed for $\delta \approx 2/3$. The same ratios for PHENIX data are plotted in the right panel of Fig. 6 where red triangles correspond to $c_2 = 20 - 40\%$, dark-green ones to $c_3 = 40 - 60\%$ and blue ones to $c_4 = 60 - 92\%$.

3.2 Energy scaling

Having established that GS is indeed achieved for $\delta = 2/3$ (or very close to $2/3$), we can now test energy scaling, *i.e.* λ dependence of GS. Unfortunately, the quality of ratios, similar to the ones defined in Eq. (8), but for different energies rather than centralities, is very poor as compared to (8). This is because the data from different experiments suffer from systematic uncertainties, like different rapidity ranges, different definition of centrality classes, etc. Therefore in Fig. 7 we simply plot spectra both for ALICE and PHENIX in terms of scaling variable τ defined in Eq. (7) for two different choices of λ : 0.2 in left panel and 0.3 in right panel. We see that it is hard to decide for which λ GS is better (with logarithmic accuracy). This shows that it is of importance to have data at different energies (at least three) from one experiment where the systematic uncertainties mentioned above cancel.

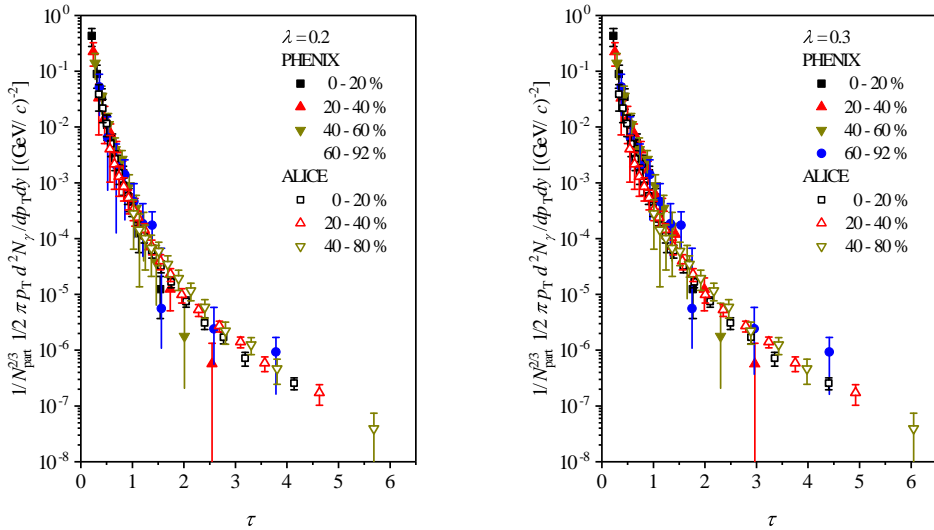


Figure 7. Illustration of geometrical scaling of the γ yields in heavy ion collisions for different centrality classes for PHENIX AuAu data at 200 GeV [20] and Alice data at 2.76 TeV [22]. Left panel: $\lambda = 0.2$, right panel $\lambda = 0.3$. Lower error bars without end caps have been arbitrarily shortened for better visibility.

4 Conclusions

Geometrical scaling is the property of the overoccupied gluonic cloud that is characterised by the new dynamical scale, called *saturation scale*. If this is the only energy scale in a given kinematical region,

then by a simple argument of dimensional analysis particle spectra should depend only on the ratio of the transverse momentum to this scale. This phenomenon has been first observed in inclusive DIS and then also in hadronic collisions. In the latter case the emergence of GS is by no means obvious due to the final state interactions, resonance decays, confinement, etc. Nevertheless GS is observed in pp scattering and also in HI collisions.

Photons that have weak final state interactions (they are rather insensitive to the QGP medium) and are free from the confinement effects seem to be a much better probe of the initial state than charged particles. This is, however, not entirely true, since photons do not couple to gluons, and therefore the fact that they still exhibit GS provides a positive test of quark production mechanism in glasma.

The analysis presented here should be carried out on the recent PHENIX data [23] including also the data obtained from the collisions of different systems (Cu+Cu [24], Au+Au [25], Pb+Pb) and small systems (p+p, d+Au, p+Au) – for review see Ref. [26].

Acknowledgements

The author acknowledges very useful discussions with Larry McLerran and Vladimir Khachatryan. This research has been supported the Polish National Science Centre grant 2014/13/B/ST2/02486.

References

- [1] A. M. Stasto, K. J. Golec-Biernat and J. Kwiecinski, *Phys. Rev. Lett.* **86**, 596 (2001)
- [2] L. McLerran, *Acta Phys. Pol. B* **41** (2010) 2799
- [3] Y. L. Dokshitzer, V. A. Khoze and S. I. Troian, *J. Phys. G* **17**, 1585 (1991)
- [4] L. McLerran and M. Praszalowicz, *Acta Phys. Pol. B* **41**, 1917 (2010)
- [5] L. McLerran and M. Praszalowicz, *Acta Phys. Pol. B* **42**, 99 (2011)
- [6] M. Praszalowicz and A. Francuz, *Phys. Rev. D* **92**, 074036 (2015)
- [7] M. Praszalowicz, *PoS DIS* **2015**, 084 (2015)
- [8] M. Praszalowicz, *Acta Phys. Pol. B Proc. Supp.* **8** 399 (2015)
- [9] M. Chiu, T. K. Hemmick, V. Khachatryan, A. Leonidov, J. Liao and L. McLerran, *Nucl. Phys. A* **900**, 16 (2013)
- [10] L. McLerran and B. Schenke, *Nucl. Phys. A* **946**, 158 (2016)
- [11] V. Khachatryan, B. Schenke, M. Chiu, A. Drees, T. K. Hemmick and N. Novitzky, *Nucl. Phys. A* **978**, 123 (2018)
- [12] C. Klein-Börsing and L. McLerran, *Phys. Lett. B* **734**, 282 (2014)
- [13] D. Kharzeev, E. Levin and M. Nardi, *Nucl. Phys. A* **747**, 609 (2005)
- [14] B. Abelev *et al.* [ALICE Collaboration], *Phys. Lett. B* **720**, 52 (2013)
- [15] J. Adams *et al.* [STAR Collaboration], *Phys. Rev. Lett.* **91**, 172302 (2003)
- [16] C. Adler *et al.* [STAR Collaboration], *Phys. Rev. Lett.* **89**, 202301 (2002)
- [17] S. S. Adler *et al.* [PHENIX Collaboration], *Phys. Rev. C* **69**, 034910 (2004)
- [18] K. Adcox *et al.* [PHENIX Collaboration], *Phys. Rev. Lett.* **88**, 022301 (2002)
- [19] A. Adare *et al.* [PHENIX Collaboration], *Phys. Rev. Lett.* **104**, 132301 (2010)
- [20] A. Adare *et al.* [PHENIX Collaboration], *Phys. Rev. C* **91**, 064904 (2015)
- [21] M. Wilde [ALICE Collaboration], *Nucl. Phys. A* **904-905**, 573c (2013)
- [22] J. Adam *et al.* [ALICE Collaboration], *Phys. Lett. B* **754**, 235 (2016)
- [23] A. Adare *et al.* [PHENIX Collaboration], arXiv:1805.04084 [hep-ex]

- [24] A. Adare *et al.* [PHENIX Collaboration], Phys. Rev. C **98**, 054902 (2018)
- [25] S. Afanasiev *et al.* [PHENIX Collaboration], Phys. Rev. Lett. **109**, 152302 (2012)
- [26] V. Khachatryan [PHENIX Collaboration], arXiv:1812.01841 [nucl-ex]